Chinese Journal of Natural Medicines

Activation of NRF2 by celastrol increases antioxidant functions and prevents the progression of osteoarthritis in mice

Mingming LIU, Jiatian GUO, Jing ZHAO, Hongye LI, Xiaoxiao FENG, Haojun LIU, Hao ZHANG, Xuejun JIA, Rushuai WEI, Fang LI, Chong CHEN, Mingzhuang HOU, Nanning LV, Haiyan XU

Citation: Mingming LIU, Jiatian GUO, Jing ZHAO, Hongye LI, Xiaoxiao FENG, Haojun LIU, Hao ZHANG, Xuejun JIA, Rushuai WEI, Fang LI, Chong CHEN, Mingzhuang HOU, Nanning LV, Haiyan XU, Activation of NRF2 by celastrol increases antioxidant functions and prevents the progression of osteoarthritis in mice, Chinese Journal of Natural Medicines, 2024, 22(2), 1−10. doi: 10.1016/S1875−5364(23)60465−0.

View online: https://doi.org/10.1016/S1875−5364(23)60465−0

Related articles that may interest you

Cyasterone inhibits IL−1 β −mediated apoptosis and inflammation *via* the NF− κ B and MAPK signaling pathways in rat chondrocytes and ameliorates osteoarthritis *in vivo*

Chinese Journal of Natural Medicines. 2023, 21(2), 99−112 https://doi.org/10.1016/S1875−5364(23)60388−7

Identification of a cytochrome P450 from *Tripterygium hypoglaucum* (Levl.) Hutch that catalyzes polpunonic acid formation in celastrol biosynthesis

Chinese Journal of Natural Medicines. 2022, 20(9), 691−700 https://doi.org/10.1016/S1875−5364(22)60205−X

Effects of chitooligosaccharide−zinc on the ovarian function of mice with premature ovarian failure *via* the SESN2/NRF2 signaling pathway

Chinese Journal of Natural Medicines. 2021, 19(10), 721−731 https://doi.org/10.1016/S1875−5364(21)60084−5

Jujuboside A ameliorates tubulointerstitial fibrosis in diabetic mice through down−regulating the YY1/TGF− β 1 signaling pathway

Chinese Journal of Natural Medicines. 2022, 20(9), 656−668 https://doi.org/10.1016/S1875−5364(22)60200−0

Dandelion polyphenols protect against acetaminophen−induced hepatotoxicity in mice *via* activation of the Nrf−2/HO−1 pathway and inhibition of the JNK signaling pathway

Chinese Journal of Natural Medicines. 2020, 18(2), 103−113 https://doi.org/10.1016/S1875−5364(20)30011−X

Effect of quercetin on chondrocyte phenotype and extracellular matrix expression

Chinese Journal of Natural Medicines. 2020, 18(12), 922−933 https://doi.org/10.1016/S1875−5364(20)60036−X

Wechat

Available online at www.sciencedirect.com
ScienceDirect
Chinese Journal of Natural Medicines 2024, **22**(2): 137-145
doi: 10.1016/S1875-5364(24)60586-8
Chinese Journal of Natural Medicines

•Original article•

Activation of NRF2 by celastrol increases antioxidant functions and prevents the progression of osteoarthritis in mice

LIU Mingming[2Δ], GUO Jiatian[2Δ], ZHAO Jing[2Δ], LI Hongye[2], FENG Xiaoxiao[2], LIU Haojun[2], ZHANG Hao[2], JIA Xuejun[2], WEI Rushuai[2], LI Fang[2], CHEN Chong[4], HOU Mingzhuang[3*], LV Nanning[2*], XU Haiyan[1*]

[1] *Department of human anatomy, Xuzhou Medical University, Xuzhou 221004, China;*
[2] *Department of Orthopedic Surgery, The Affiliated Lianyungang Clinical College of Xuzhou Medical University (The Second People's Hospital of Lianyungang), Lianyungang 222003, China;*
[3] *Department of Orthopaedics, The First Afliated Hospital of Soochow University, Soochow University, Suzhou 215006, China;*
[4] *Institute of Hematology, Xuzhou Medical University, Xuzhou 221004, China*

Available online 20 Feb., 2024

[ABSTRACT] Excessive oxidative stress impairs cartilage matrix metabolism balance, significantly contributing to osteoarthritis (OA) development. Celastrol (CSL), a drug derived from *Tripterygium wilfordii*, has recognized applications in the treatment of cancer and immune system disorders, yet its antioxidative stress mechanisms in OA remain underexplored. This study aimed to substantiate CSL's chondroprotective effects and unravel its underlying mechanisms. We investigated CSL's impact on chondrocytes under both normal and inflammatory conditions. *In vitro*, CSL mitigated interleukin (IL)-1β-induced activation of proteinases and promoted cartilage extracellular matrix (ECM) synthesis. *In vivo*, intra-articular injection of CSL ameliorated cartilage degeneration and mitigated subchondral bone lesions in OA mice. Mechanistically, it was found that inhibiting nuclear factor erythroid 2-related factor 2 (NRF2) abrogated CSL-mediated antioxidative functions and exacerbated the progression of OA. This study is the first to elucidate the role of CSL in the treatment of OA through the activation of NRF2, offering a novel therapeutic avenue for arthritis therapy.

[KEY WORDS] Osteoarthritis; Celastrol; Articular cartilage; Extracellular matrix; NRF2
[CLC Number] R965 **[Document code]** A **[Article ID]** 2095-6975(2024)02-0137-09

Introduction

Osteoarthritis (OA), a leading cause of adult disability, is a chronic musculoskeletal disease characterized by cartilage degeneration, synovitis, subchondral osteosclerosis, and osteophyte formation [1]. Beyond its significant health implications, OA exerts a profound impact on the socio-economic landscape [2]. The prevalence of OA is on an upward trajectory, exacerbated by the aging global population and increasing obesity rates, positioning it as the fourth leading cause of disability worldwide. OA manifests as a comprehensive joint disease, affecting various structures including cartilage, subchondral bone, ligaments, synovium, and muscles surrounding the joint [3]. The clinical presentation of OA is dominated by pain, accompanied by morning stiffness, diminished range of motion, joint instability, swelling, muscle weakness, fatigue, and psychological distress related to pain [4]. Fundamentally, OA is characterized by the progressive degeneration of the cartilage extracellular matrix (ECM), where key components such as collagen II (COL II) and aggrecan are crucial for maintaining the metabolic balance of cartilage and resisting mechanical stresses. In OA, however, there is a pathological increase in the release of degradative enzymes, notably a disintegrin metalloproteinase with thrombospondin motifs 5 (ADAMTS5) and matrix metalloproteinase-13 (MMP-13), by dysfunctional chondrocytes, further accelerating the deterioration of articular cartilage [5].

Oxidative stress, a key player in arthritis pathology, disrupts the essential matrix metabolism vital for chondrocyte survival. Notably, an overproduction of reactive oxygen species (ROS) has been linked to the induction of chondrocyte

[Received on] 26-Aug.-2023
[Research funding] This work was supported by the Key Research and Development Plan of Jiangsu Province (Social Development Project, No. BE2021679) and the National Natural Science Foundation Project (No. 82171762).
[*Corresponding author] E-mails: xhy_8@163.com (XU Haiyan); lvnanning123@163.com (LV Nanning); houmingzhuangyll@163.com (HOU Mingzhuang)
[Δ]These authors contributed equally to this work.
These authors have no conflict of interest to declare.

apoptosis [6]. Furthermore, these elevated ROS levels compromise the antioxidant defense system of chondrocytes, increasing their vulnerability to oxidative stress. This aberrant increase in ROS not only triggers cell death *via* apoptosis, necrosis, and autophagy but also promotes ECM degradation through the upregulation of MMPs and ADAMTs [7]. Nuclear factor E2 related factor 2 (NRF2), a widely functional transcriptional activator, is closely related to the redox homeostasis of cells [8]. Studies have demonstrated its capacity to regulate cytoprotective targets, significantly enhancing cellular resistance to oxidative stress [9-10].

Celastrol (CSL), a compound extracted from the root of *Tripterygium wilfordii*, has been traditionally used in China for treating a variety of inflammatory diseases. Recognized for its potent anti-inflammatory and antioxidant properties, CSL has been employed in the management of rheumatoid arthritis (RA), systemic lupus erythematosus, and various cancers [11-13]. We hypothesized that CSL inhibits ECM degeneration in OA cartilage by enhancing the antioxidant defense of chondrocytes. To evaluate the positive effects of CSL on preventing cartilage degeneration, we injected it intra-articularly into OA mice. Furthermore, this study explored CSL's impact on the NRF2 signaling pathway and its modulation of antioxidant cytokines.

Materials and Methods

Cell isolation and culture

All animal experiments were approved by the Ethics Committee of Xuzhou Medical University (202211A263). Articular cartilage tissues were harvested from C57BL/6 mice, followed by dissection using a sterile scalpel. For cell digestion, the tissues were treated with a 2 mg·mL^{-1} collagenase solution and incubated for 6 h. Subsequently, the solution was filtered by sterile screens (100 μm) to remove undigested tissue residues. The resulting chondrocytes were cultured in DMEM/F12 at 37 °C in a 5% CO_2 incubator. For consistency in experimental procedures, second-generation (P2) chondrocytes were exclusively employed in subsequent experiments.

Treatment with IL-1β, CSL, and ML385

To simulate an *in vitro* OA inflammatory microenvironment, chondrocytes were incubated with recombinant IL-1β (10 ng·mL^{-1}). Celastrol (CSL, NSC 70931, Selleck, TX, USA) was prepared in 10 and 20 μmol·L^{-1} for use in medium dilutions. Additionally, chondrocytes were exposed to ML385 (5 μmol·L^{-1}, Topscience, Shanghai, China), a specific NRF2 inhibitor, to inhibit the NRF2 activity. Nrf2 siRNA (siNrf2) (sense: 5′-GGUUGAGACUACCAUGGUUTT-3′, anti-sense: 5′-AACCAUGGUAGUCUCAACCTT-3′) and negative control (NC) (sense: 5′-UUCUCCGAACGUGUCACGUTT-3′, anti-sense: 5′-ACGUGACACGUUCGGAGAATT-3′) were synthesized by Tsingke Biotechnology (Beijing, China).

Cell proliferation

Cell proliferation was detected by Cell Counting Kit-8 assay (CCK-8, Beyotime, Haimen, China). The isolated chondrocytes were seeded in a 96-well plate at a density of 3000 cells per well and treated with 10 or 20 μmol·L^{-1} CSL. On days 1, 3, 5, and 7, cells were incubated with the CCK-8 working solution in the dark at 37 °C for 1 h. The absorbance at 450 nm was measured using a microplate reader (BioTek, Winooski, VT, USA).

Immunofluorescence assay

The immunofluorescence process commenced with fixing chondrocytes using 4% paraformaldehyde (Beyotime, China). Following fixation, the chondrocytes were permeabilized in 0.1% Triton X-100 (Beyotime) for 30 min and blocked using a specific blocking solution (Beyotime) at room temperature for 20 min. Subsequently, the cells were incubated with diluted antibodies (anti-COL II, ab34712, anti-NRF2, ab62352; Abcam, Cambridge, MA, USA) overnight at 4 °C. After rinsing with PBS thrice, the chondrocytes were incubated with fluorescent secondary antibodies (ab150083, Abcam). Finally, 4′,6-diamidino-2-phenylindole (DAPI, Beyotime) was used for nuclear staining. Immunofluorescent images were captured and examined under a fluorescent microscope (Zeiss, Oberkochen, Germany), enabling the visualization of protein expression within the chondrocytes.

Western blotting assay

Total protein was extracted from chondrocytes using radioimmunoprecipitation assay (RIPA) lysis buffer (Beyotime). Protein concentration was measured using the bicinchoninic acid (BCA) kit (Beyotime, China). Equal amounts of protein were subjected to SDS-PAGE (Beyotime, China). Following electrophoretic separation, proteins were transferred onto nitrocellulose membranes (Beyotime, China). The membranes were blocked for 30 min and subsequently incubated overnight at 4 °C with various diluted primary antibodies: anti-COL II (ab34712), anti-ACAN (ab3778), anti-heme oxygenase-1 (HO-1, ab137550), anti-SOD1 (ab13498), anti-MMP13 (ab51072), anti-NRF2 (ab137550), anti-ADAMTS5 (ab182795), anti-GPX1 (ab108429), anti-CAT (ab209211), and anti-F-actin (ab130935). Thereafter, the membranes were incubated with horseradish peroxidase (HRP)-conjugated secondary antibody (ab288151) for 1 h. Post-incubation, the membranes were washed and exposed to 3 mL of chemiluminescent substrate (Thermo Fisher Scientific, MA, USA), and the protein bands were visualized on an imaging system (Bio-Rad, CA, USA). The optical density of the bands was quantified using Image-J software (National Institutes of Health, Bethesda, MD, USA).

Quantitative real-time reverse transcription-polymerase chain reaction (RT-PCR)

The gene expression levels of *Col2a1*, *Acan*, *Adamts5*, *Mmp13*, *Nrf2*, *Hmox1*, *Gpx1*, *Catalase*, and *Sod1* in the chondrocytes of each group were detected by real-time RT-PCR with *Gapdh* as the internal control. Primer sequences are detailed in Supplementary Table 1. Total RNA was extracted

from the chondrocytes using TRIzol reagent (Beyotime, China), and RT-PCR was performed using the SYBR Green Supermix kit in a CFX96TM PCR instrument (Bio-Rad, Hercules, CA, USA). The mRNA expression levels were calculated using the ΔC_t method ($2^{-\Delta\Delta C_t}$).

OA model induction by the destabilization of the medial meniscus (DMM) surgery and animal treatment

All animal experiments were approved by the Ethics Committee of Xuzhou Medical University (202211A263). DMM surgery was performed to establish an OA model in 8-week-old C57BL/6J mice (male, weight 20−25 g). After the administration of sodium pentobarbital for anesthesia, the medial meniscotibial ligaments (MML) of mice were transected. The mice were divided into four groups: (1) Sham group: the knee joint capsules were incised without any further treatment; (2) DMM group: the joint capsules were incised and injected with saline; (3) CSL group: the joint capsules were incised and treated with intraperitoneal CSL (0.1 mg·kg^{-1}) for 14 days; and (4) CSL + ML385 group: the mice were administered CSL (0.1 mg·kg^{-1}) and ML385 (10 μL of 100 mmol·L^{-1}) for 14 days.

Micro-computed tomography (μCT) analysis

Subchondral bone mass was quantitatively assessed μCT (Skyscan 1176, Kontich, Belgium) at 50 kV (200 μA). The subchondral parameters of interest were calculated and analyzed, including trabecular separation (Tb.Sp., mm) and bone volume fraction (BV/TV, %).

Histological staining

For histological evaluations, the collected samples were first fixed in 10% formalin and decalcified with 14% ethylenediamine tetraacetic acid (EDTA) for eight weeks. Post-decalcification, the samples were embedded in paraffin and cut into sections (5 μm). These sections were then stained with Safranin O/Fast Green (Jiancheng Bioengineering Institute, Nanjing, China). Microscopic examination and imaging of the stained tissues were conducted using a microscope (Zeiss).

Statistical analysis

Data were analyzed using SPSS 19.0 software (IBM Corporation, Armonk, NY, USA). The statistical method employed was the one-way analysis of variance (ANOVA), complemented by an unpaired two-sample Student's *t*-test for determining the significance of differences. $P < 0.05$ indicated statistically significant differences.

Results

CSL inhibited cartilage matrix degradation

The impact of CSL on chondrocyte proliferation and car-

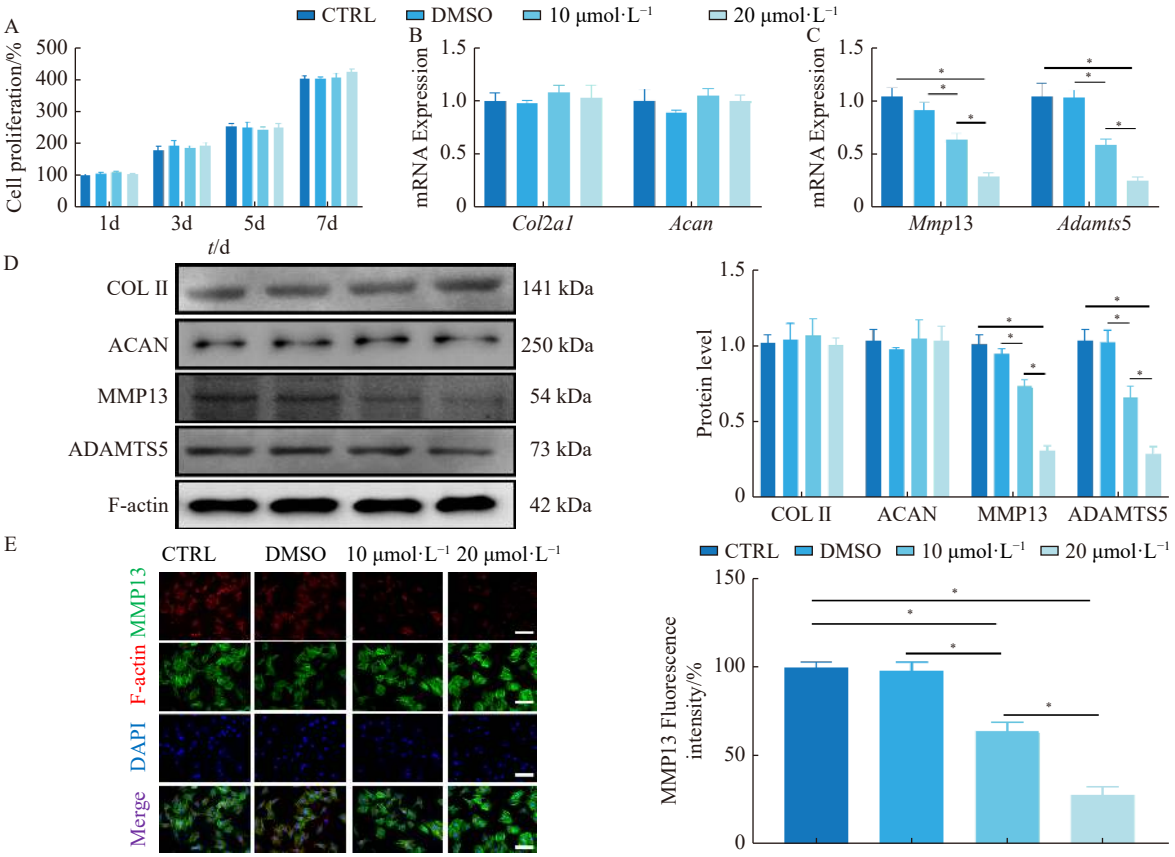

Fig. 1 Effects of CSL on the proliferation of chondrocytes under normal culture conditions. (A) Proliferation of chondrocytes after 1, 3, 5, and 7 days of CSL treatment. (B, C) RT-PCR analysis for the mRNA expression levels of *Col2a1*, *Acan*, *Mmp13*, and *Adamts5*. (D) Effects of CSL on the protein levels of COL II, ACAN, MMP13, and ADAMTS5. (E) Immunofluorescence assay for the expression of MMP13 (Scale bar = 100 μm). Data are presented as the mean ± SD ($n = 4$), $^*P < 0.05$.

tilage ECM synthesis was assessed using a Cell Counting Kit-8 (CCK-8) assay. The results demonstrated that CSL at concentrations 10 and 20 μmol·L^{-1} had no significant impact on cell proliferation. Furthermore, the transcriptional expression levels of *Col2a1* and *Acan* remained unaltered following treatment with CSL (Figs. 1A and 1B). Western blot analysis further confirmed that the protein expression levels of COL II and ACAN were not notably influenced by CSL treatment (Fig. 1D). These observations imply that CSL does not markedly enhance cartilage ECM synthesis under non-inflammatory conditions. Contrastingly, CSL exhibited a concentration-dependent suppression of genes associated with matrix degradation, specifically *Mmp13* and *Adamts5* (Fig. 1C). This inhibitory effect of CSL was further substantiated by immunofluorescence and Western blotting assays, which showed a reduction in the protein expression levels of ADAMTS5 and MMP13 (Figs. 1D and 1E).

CSL ameliorated IL-1β-induced metabolic imbalance in chondrocytes

The results of the CCK-8 assay showed that CSL at concentrations of 10 and 20 μmol·L^{-1} mitigated IL-1β-induced apoptosis in chondrocytes. IL-1β treatment decreased cell proliferation by 25.25% on day 7 compared with the proliferation of the control groups. It is worth noting that the ability of CSL to reverse the negative effects of IL-1β on cell proliferation increased with time. On day 7, the proliferation abilities of the chondrocytes in the 20 μmol·L^{-1} CSL groups were almost the same as that of the control groups (Fig. 2A). Quantitative RT-PCR analysis demonstrated that IL-1β significantly reduced the mRNA expression levels of *Col2a1* and *Acan*. Conversely, CSL treatment increased the transcriptional levels of these genes relative to the IL-1β group (Fig. 2B). Furthermore, 10 and 20 μmol·L^{-1} CSL showed a concentration-dependent inhibition of genes associated with matrix degradation, including *Mmp13* and *Adamts5* (Fig. 2C). The Western blotting assay corroborated CSL's dose-dependent protective effects on the metabolic homeostasis of cartilage ECM at the protein level (Fig. 2D). The immunofluorescence assay revealed that IL-1β disrupted the metabolic homeostasis of the ECM, while the treatment of CSL countered this disruption. CSL not only augmented matrix synthesis but also reduced the expression of matrix-degrading enzymes (Fig. 2E).

CSL enhanced chondrocyte antioxidant capacity for cartilage protection

This study further investigated CSL's protective mechanism on cartilage by examining oxidative stress parameters in chondrocytes, specifically reactive oxygen species (ROS)

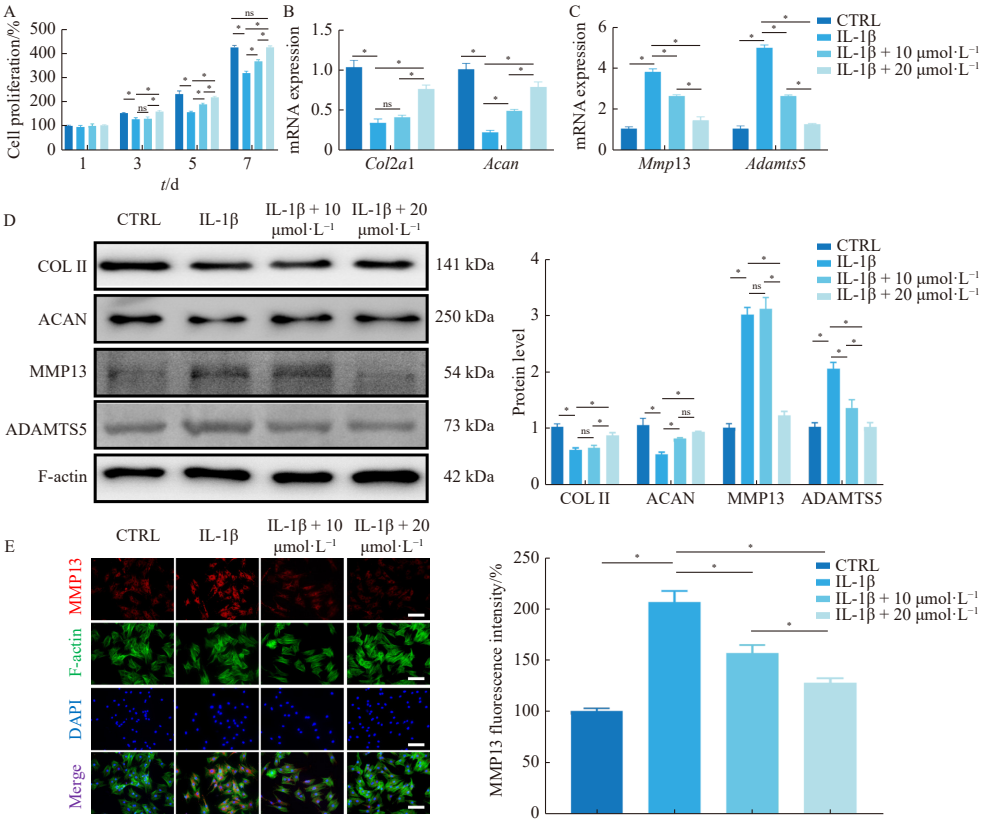

Fig. 2 Effects of CSL on the proliferation of chondrocytes under inflammatory conditions induced by IL-1β. (A) Proliferation of chondrocytes after 1, 3, 5, and 7 days of CSL and IL-1β treatment. (B, C) RT-PCR analysis for the mRNA expression levels of *Col2a1*, *Acan*, *Mmp13*, and *Adamts5*. (D) Effects of CSL on the protein levels of COL II, ACAN, MMP13, and ADAMTS5. (E) Immunofluorescence assay for the expression of MMP13 (Scale bar = 100 μm). Data are presented as the mean ± SD (n = 4), $^*P$ < 0.05.

levels and antioxidant markers, following treatment with CSL and IL-1β. It was observed that 20 μmol·L^{-1} CSL decreased the excessive ROS proliferation induced by IL-1β (Fig. 3A). In addition, CSL treatment led to an upregulation at the gene expression level of several key antioxidant enzymes, including *Hmox1*, *Sod1*, *Cat*, and *Gpx1* (Figs. 3B−3E). Meanwhile, an increase in the protein expression of these enzymes was also observed post-CSL treatment (Figs. 3F−3J).

CSL enhanced the antioxidant capacity of chondrocytes by activating the NRF2 axis

This study investigated the involvement of the NRF2 axis in the CSL-mediated enhancement of antioxidant capacity in chondrocytes. It was observed that IL-1β exposure led to a decrease in NRF2 expression at both gene and protein levels. In contrast, CSL treatment effectively counteracted this IL-1β-induced impairment of NRF2 (Figs. 4A and 4B). When the chondrocytes were exposed to ML385 or siNRF2, the expression of NRF2 was blocked significantly, and the nuclear translocation of NRF2 was prevented (Figs. 4C and 4D). Under these inhibitory conditions, CSL's positive effects were markedly diminished or entirely negated. This observation was further substantiated by the Western blotting assay, revealing that NRF2 knockdown *via* ML385 or siNRF2 disrupted the balance of ECM metabolism and reduced the efficacy of CSL (Fig. 4E, Supplementary Figs. 1A−1C). Additionally, RT-PCR results supported these findings, demonstrating a reduced effectiveness of CSL in the presence of siNRF2. This outcome emphasized the role of CSL in modulating matrix metabolism predominantly through NRF2 activation (Figs. 4F−4H).

CSL prevented cartilage degeneration in OA mice

Safranin O and fast green staining showed that CSL preserved the cartilage structure and impeded the loss of glycosaminoglycans (GAGs) in OA mice. However, treatment with ML385, an NRF2 inhibitor, negated CSL's beneficial effects on the cartilage ECM, thereby accelerating the progression of OA (Figs. 5A and 5B). The coronal images captured by μCT identified that CSL treatment ameliorated the subchondral bone loss, and ML385 weakened the protective effect of CSL in OA mice (Fig. 5C). This finding was further quantified by μCT analysis, with parameters such as bone volume ratio (BV/TV, %) and trabecular separation (Tb.Sp., mm) indicating that CSL effectively prevented subchondral bone lesions, a benefit that was compromised by ML385 (Figs. 5D and 5E). In summary, these findings collectively suggest that CSL not only counteracts articular cartilage de-

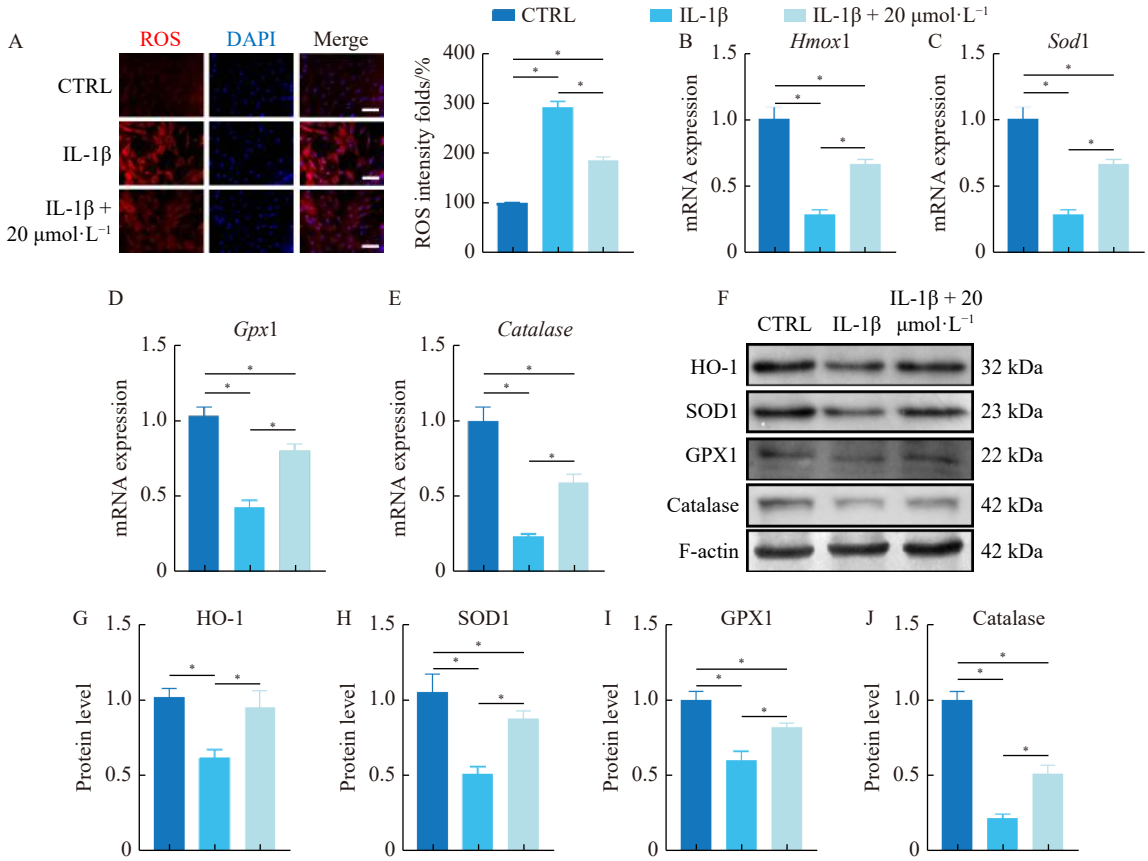

Fig. 3 CSL enhanced the antioxidant capacity of chondrocytes under inflammatory conditions induced by IL-1β. (A) Effects of CSL on the amount of ROS in chondrocytes. (B−E) RT-PCR analysis for the mRNA expression of *Hmox1*, *Sod1*, *Catalase*, and *Gpx1*. (F−J) The effects of CSL on the protein levels of HO-1, SOD1, Catalase, and GPX1 (Scale bar = 100 μm). The data are presented as the mean ± SD (n = 4), $^{*}P < 0.05$.

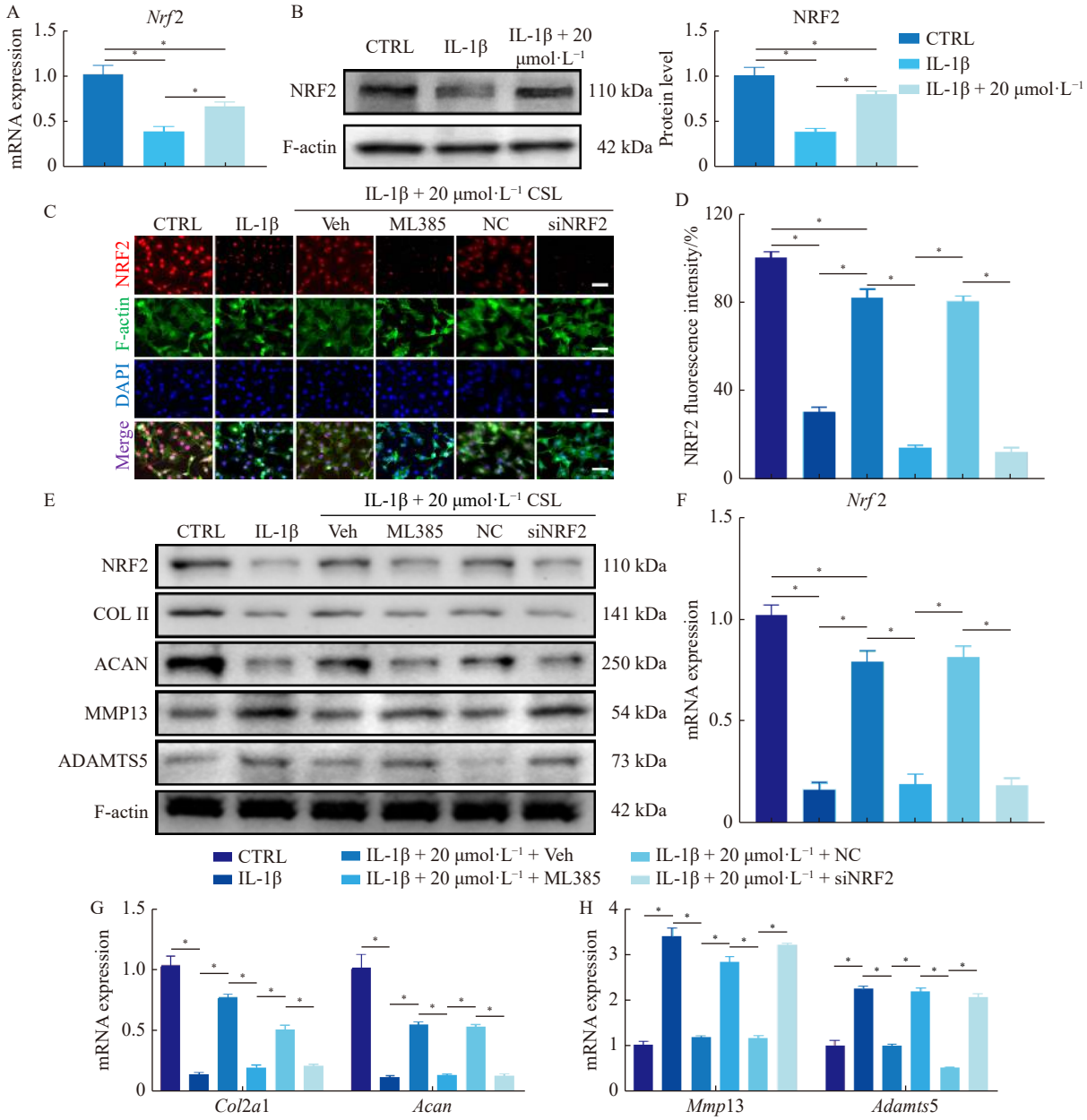

Fig. 4 CSL regulated matrix synthesis and degradation metabolism *via* the activation of NRF2. (A) Effects of CSL on the mRNA level of *Nrf2*. (B) Effects of CSL on the protein level of NRF2. (C, D) Immunofluorescence assay for the expression of NRF2. (E) Western blotting assay for the protein expression levels of NRF2, COL II, ACAN, MMP13, and ADAMTS5. (F−H) RT-PCR analysis for the mRNA expression levels of *Nrf2*, *Col2a1*, *Acan*, *Mmp13*, and *Adamts5* (Scale bar = 100 μm). Data are presented as the mean ± SD ($n = 4$), $^{*}P < 0.05$.

gradation induced by DMM surgery but also mitigates subchondral bone lesions *via* the activation of NRF2. The expressions of the representative markers for matrix synthesis (COL II), matrix degradation (MMP13), and oxidative stress (SOD1) were detected by immunohistochemical staining. In addition, as a direct downstream target of NRF2, the expression of HO-1 was also detected *in vivo*. The results indicated that ML385 could disrupt the ECM metabolic homeostasis maintained by CSL, exhibiting the ability to increase the expression of MMP13 and reduce the expression of COL II (Figs. 6A−6C). The expression levels of SOD1 and HO-1 were also up-regulated by CSL, while ML385 weakened this protective effect of CSL (Figs. 6A, 6D and 6E).

Discussion

While the roles of key pro-inflammatory cytokines, such as TNF-α and IL-1β, are well-documented in the pathogenesis of OA, significantly influencing its incidence and progression, the comprehensive pathogenesis of OA remains not fully understood [14]. In recent years, increasing evidence has indicated that abnormal ROS levels play a significant role in the occurrence and development of OA [15]. ROS induces

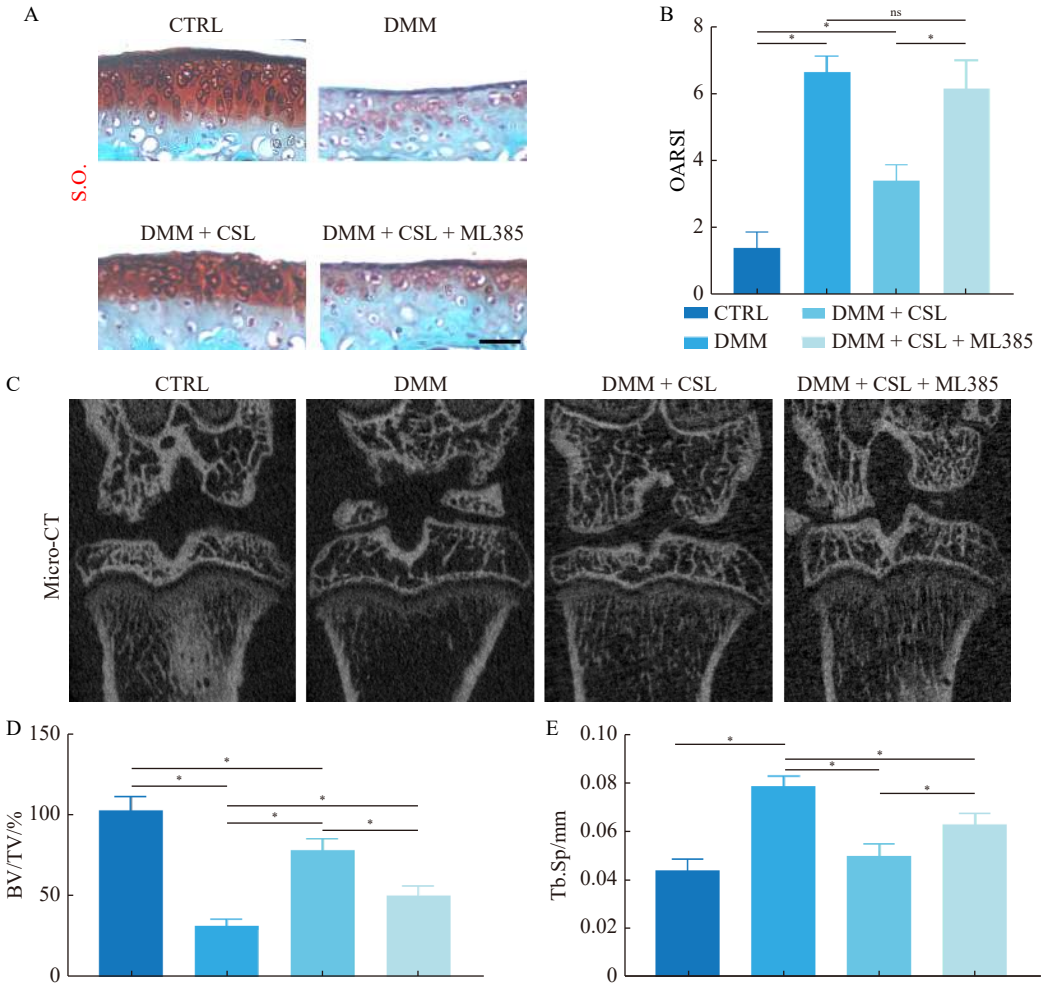

Fig. 5 CSL inhibited the progression of OA and prevented ECM synthesis, degradation, and metabolism *via* activating NRF2. (A) Representative images of articular cartilage stained by safranin O and fast green. (B) OARSI scores based on safranin O and fast green staining. (C) Micro-CT images of coronal planes of the femoral condyle and tibial plateau in OA mice. The effects of CSL on the subchondral bone health-related parameters, including (D) the bone volume ratio (BV/TV, %) and (E) trabecular separation (Tb.Sp., mm) (Scale bar = 100 μm). Data are presented as the mean ± SD (n = 4), $^{*}P$ < 0.05.

chondrocyte apoptosis by regulating p38 and c-Jun *N*-terminal kinase (JNK) signaling pathways [16]. Moreover, ROS impairs the antioxidant defense system of chondrocytes, thereby increasing their sensitivity to oxidative stress [17]. The excessive ROS, particularly induced by IL-1β, contributes not only to the degradation of chondrocytes' ECM but also intensifies this degradation by upregulating MMPs and reducing the production of tissue inhibitors of metalloproteinases [18].

CSL, a pentacyclic triterpene, is renowned for its robust anti-inflammatory and antioxidant properties [19, 20]. It has been widely employed in treating conditions such as rheumatoid arthritis (RA), systemic lupus erythematosus (SLE), and various cancers [21]. The anti-inflammatory and antioxidant mechanisms of CSL are thought to involve reducing inducible NO synthase-dependent peroxynitrite, promoting the heat shock response, and enhancing autophagy [22, 23]. Recent studies have shown that CSL protects human chondrocytes by downregulating the expression of pro-inflammatory cytokines [24] and alleviates pain and cartilage damage in OA through modulating the SDF-1 and TLR2/NF-κB signaling pathway [25, 26]. Furthermore, CSL treatment has been observed to remarkably reduce the expression of cleaved caspase-3 and Bax while reversing the Bcl-2 impairment induced by IL-1β in chondrocytes [27]. Consistent with these previous studies [22-27], our research further confirmed the positive effects of CSL. We demonstrated that CSL preserved the metabolic balance of cartilage ECM and prevented articular cartilage degeneration in OA.

NRF2 is a transcription control factor abundantly present in the human body, playing a crucial role in the antioxidant defense system. It is well-acknowledged that the nuclear translocation of NRF2 activates its pathway, thereby modulating antioxidant enzymes in various mammals [28]. Recently, the critical role of NRF2 in maintaining cartilage ECM homeostasis has garnered increased attention. Studies have demonstrated that NRF2 is vital for preserving the stability of

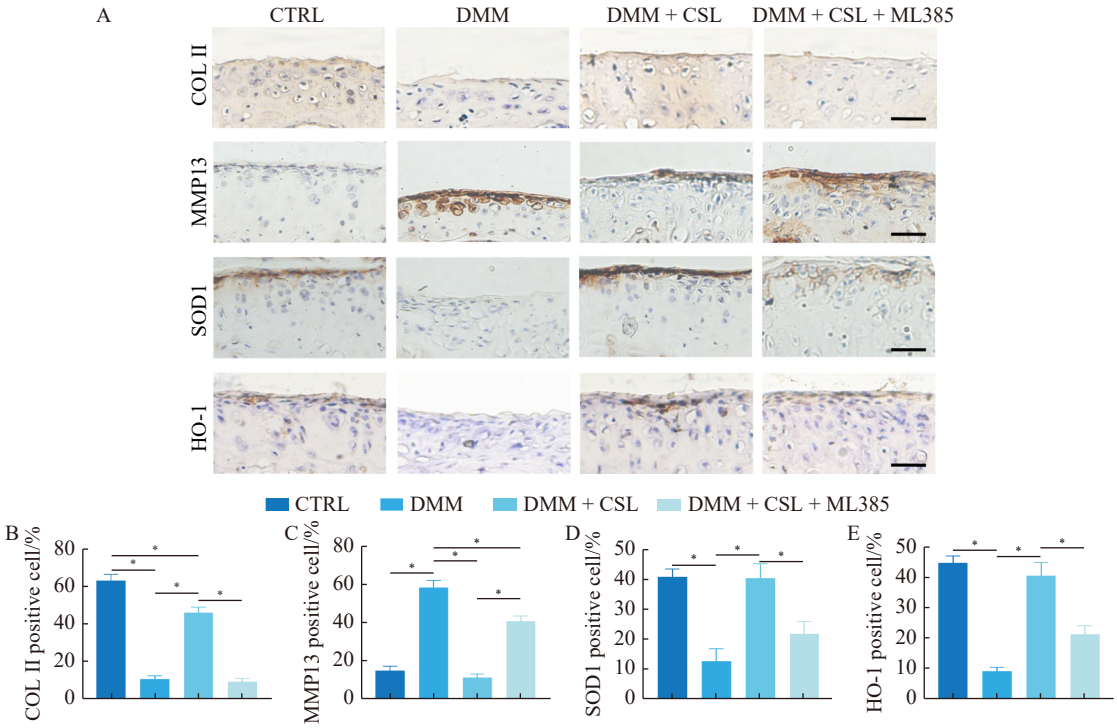

Fig. 6 CSL regulated the metabolic balance of cartilage ECM and increased the expression of antioxidant enzymes. (A) Representative images of immunohistochemistry of COL II, MMP13, SOD1, and HO-1 in articular cartilage (Scale bar = 100 μm). (B) Quantitative analysis of COL II positive cells. (C) Quantitative analysis of MMP13 positive cells. (D) Quantitative analysis of SOD1 positive cells. (E) Quantitative analysis of HO-1 positive cells. Data are presented as the mean ± SD (n = 4), $^{*}P < 0.05$.

articular cartilage, ensuring a balance between matrix synthesis and degradation [29]. NRF2 activation can upregulate the expression of HO-1, thereby enhancing ECM synthesis, inhibiting chondrocyte apoptosis, and protecting cartilage tissue [30]. Research by ZHANG *et al*. has revealed that NRF2 knockout mice develop OA more rapidly post-DMM surgery than wild-type mice [31]. Furthermore, existing studies have elucidated that NRF2 not only suppresses the production of inducible nitric oxide synthase and cyclooxygenase-2 in the inflammatory milieu of OA but also plays a pivotal role in delaying cartilage degeneration by inhibiting matrix-degrading enzymes and increasing the expression of anti-apoptotic proteins [32].

The protective effects of various antioxidants on cartilage, such as resveratrol [33], androgen Liannei [34], and red sandalwood root [35], have been strongly associated with the NRF2 signaling pathway. In this study, we observed that CSL also played an antioxidant role by activating the NRF2 pathway and its downstream genes related to antioxidant activities. CSL downregulated the levels of ROS and matrix-degrading enzymes, which were initially stimulated by IL-1β. Notably, this effect was attenuated when the chondrocytes were exposed to the inhibitor of NRF2 (ML385). Furthermore, we demonstrated that CSL treatment not only alleviated the lesions of subchondral bone but also enhanced OA cartilage integrity by improving the expression levels of COL II and GAG. ML385 intervention aggravated the symptoms of arthritis, a finding consistent with our *in vitro* experimental results.

Our study is the first to detail the cartilage-protective effects of CSL on the ECM. CSL mitigates the activity of matrix-degrading enzymes in chondrocytes, addressing the disruption in matrix metabolism caused by inflammatory environments. While existing literature predominantly focuses on CSL's anti-inflammatory actions in treating OA [24], our research uniquely identifies its role in enhancing antioxidant capacity and activating the NRF2 pathway. We discovered that CSL elevated the expression of antioxidant enzymes, significantly reducing ROS levels induced by IL-1β. *In vivo*, the intra-articular injection of CSL decelerated OA progression, curbed the loss of glycosaminoglycans, and safeguarded the cartilage ECM. However, the introduction of an NRF2-specific inhibitor (ML385 and siRNA) notably weakened CSL's antioxidative efficacy.

In conclusion, our findings demonstrate CSL's antioxidative and chondroprotective effects both *in vivo* and *in vitro*, primarily through the upregulation of the NRF2 pathway. CSL effectively inhibits the release of ROS and prevents cartilage degradation, underscoring its potential as a valuable therapeutic option in OA treatment. This study paves the way for novel therapeutic approaches in OA management, meriting further exploration in future research endeavors.

References

[1] Pigeolet M, Jayaram A, Park KB, *et al*. Osteoarthritis in 2020 and beyond [J]. *Lancet*, 2021, **397**(10279): 1059-1060.

[2] Tang X, Wang S, Zhan S, *et al*. The prevalence of symptomatic knee osteoarthritis in China: results from the China health and retirement longitudinal study [J]. *Arthritis Rheumatol*, 2016, **68**(3): 648-53.
[3] Phillips RE. Review of hip and knee osteoarthritis [J]. *JAMA*, 2021, **325**(24): 2504-2505.
[4] Roos EM, Herzog W, Block JA, *et al*. Muscle weakness, afferent sensory dysfunction and exercise in knee osteoarthritis [J]. *Nat Rev Rheumatol*, 2011, **7**(1): 57-63.
[5] Chen D, Shen J, Zhao W, *et al*. Osteoarthritis: toward a comprehensive understanding of pathological mechanism [J]. *Bone Res*, 2017, **5**: 16044.
[6] Nelson KJ, Bolduc JA, Wu H, *et al*. $H_{(2)}O_{(2)}$ oxidation of cysteine residues in c-Jun *N*-terminal kinase 2 (JNK2) contributes to redox regulation in human articular chondrocytes [J]. *J Biol Chem*, 2018, **293**(42): 16376-16389.
[7] Sun K, Jing X, Guo J, *et al*. Mitophagy in degenerative joint diseases [J]. *Autophagy*, 2021, **17**(9): 2082-2092.
[8] LeBoeuf SE, Wu WL, Karakousi TR, *et al*. Activation of oxidative stress response in cancer generates a druggable dependency on exogenous non-essential amino acids [J]. *Cell Metab*, 2020, **31**(2): 339-350.e4.
[9] Okazaki K, Anzawa H, Liu Z, *et al*. Enhancer remodeling promotes tumor-initiating activity in NRF2-activated non-small cell lung cancers [J]. *Nat Commun*, 2020, **11**(1): 5911.
[10] Cuadrado A, Rojo AI, Wells G, *et al*. Therapeutic targeting of the NRF2 and KEAP1 partnership in chronic diseases [J]. *Nat Rev Drug Discov*, 2019, **18**(4): 295-317.
[11] Yang N, Li M, Wu L, *et al*. Peptide-anchored neutrophil membrane-coated biomimetic nanodrug for targeted treatment of rheumatoid arthritis [J]. *J Nanobiotechnol*, 2023, **21**(1): 13.
[12] Liu Y, Li J. Self-assembling nanoarchitectonics of size-controllable celastrol nanoparticles for efficient cancer chemotherapy with reduced systemic toxicity [J]. *J Colloid Interface Sci*, 2023, **636**: 216-222.
[13] Song XQ, Yu Z, Yang NN, *et al*. Molecular mechanism of celastrol in the treatment of systemic lupus erythematosus based on network pharmacology and molecular docking technology [J]. *Life Sci*, 2020, **240**: 117063.
[14] Schroder A, Nazet U, Muschter D, *et al*. Impact of mechanical load on the expression profile of synovial fibroblasts from patients with and without osteoarthritis [J]. *Int J Mol Sci*, 2019, **20**(3): 585.
[15] Zhou X, Zhang Y, Hou M, *et al*. Melatonin prevents cartilage degradation in early-stage osteoarthritis through activation of miR-146a/NRF2/HO-1 axis [J]. *J Bone Miner Res*, 2022, **37**(5): 1056-1072.
[16] Bolduc JA, Collins JA, Loeser RF. Reactive oxygen species, aging and articular cartilage homeostasis [J]. *Free Radic Biol Med*, 2019, **132**: 73-82.
[17] Shen C, Cai GQ, Peng JP, *et al*. Autophagy protects chondrocytes from glucocorticoids-induced apoptosis *via* ROS/Akt/FOXO3 signaling [J]. *Osteoarthr Cartilage*, 2015, **23**(12): 2279-2287.
[18] Busa P, Lee SO, Huang N, *et al*. Carnosine alleviates knee osteoarthritis and promotes synoviocyte protection *via* activating the Nrf2/HO-1 signaling pathway: an *in-vivo* and *in-vitro* study [J]. *Antioxidants (Basel)*, 2022, **11**(6): 1209.
[19] Kannaiyan R, Shanmugam MK, Sethi G. Molecular targets of celastrol derived from thunder of god vine: potential role in the treatment of inflammatory disorders and cancer [J]. *Cancer Lett*, 2011, **303**(1): 9-20.
[20] Chen XC, Lu Y, Liu Y, *et al*. Identification of a cytochrome P450 from *Tripterygium hypoglaucum* (Levl.) Hutch that catalyzes polpunonic acid formation in celastrol biosynthesis [J]. *Chin J Nat Med*, 2022, **20**(9): 691-700.
[21] Corson TW, Crews CM. Molecular understanding and modern application of traditional medicines: triumphs and trials [J]. *Cell*, 2007, **130**(5): 769-774.
[22] Venkatesha SH, Astry B, Nanjundaiah SM, *et al*. Suppression of autoimmune arthritis by celastrus-derived celastrol through modulation of pro-inflammatory chemokines [J]. *Bioorg Med Chem*, 2012, **20**(17): 5229-5234.
[23] Deng YN, Shi J, Liu J, *et al*. Celastrol protects human neuroblastoma SH-SY5Y cells from rotenone-induced injury through induction of autophagy [J]. *Neurochem Int*, 2013, **63**(1): 1-9.
[24] Wang W, Ha C, Lin T, *et al*. Celastrol attenuates pain and cartilage damage *via* SDF-1/CXCR4 signalling pathway in osteoarthritis rats [J]. *J Pharm Pharmacol*, 2018, **70**(1): 81-88.
[25] Yang G, Wang K, Song H, *et al*. Celastrol ameliorates osteoarthritis *via* regulating TLR2/NF-kappaB signaling pathway [J]. *Front Pharmacol*, 2022, **13**: 963506.
[26] Ding QH, Cheng Y, Chen WP, *et al*. Celastrol, an inhibitor of heat shock protein 90beta potently suppresses the expression of matrix metalloproteinases, inducible nitric oxide synthase and cyclooxygenase-2 in primary human osteoarthritic chondrocytes [J]. *Eur J Pharmacol*, 2013, **708**(1-3): 1-7.
[27] Feng K, Chen H, Xu C. Chondro-protective effects of celastrol on osteoarthritis through autophagy activation and NF-kappaB signaling pathway inhibition [J]. *Inflamm Res*, 2020, **69**(4): 385-400.
[28] Kim KH, Son JM, Benayoun BA, *et al*. The mitochondrial-encoded peptide MOTS-c translocates to the nucleus to regulate nuclear gene expression in response to metabolic stress [J]. *Cell Metab*, 2018, **28**(3): 516-524.e7.
[29] Khan NM, Ahmad I, Haqqi TM. Nrf2/ARE pathway attenuates oxidative and apoptotic response in human osteoarthritis chondrocytes by activating ERK1/2/ELK1-P70S6K-P90RSK signaling axis [J]. *Free Radic Biol Med*, 2018, **116**: 159-171.
[30] Peng YJ, Lu JW, Lee CH, *et al*. Cardamonin attenuates inflammation and oxidative stress in interleukin-1beta-stimulated osteoarthritis chondrocyte through the Nrf2 pathway [J]. *Antioxidants (Basel)*, 2021, **10**(6): 862.
[31] Zhang Q, Bai X, Wang R, *et al*. 4-Octyl itaconate inhibits lipopolysaccharide (LPS)-induced osteoarthritis *via* activating Nrf2 signalling pathway [J]. *J Cell Mol Med*, 2022, **26**(5): 1515-1529.
[32] Wang Y, Chen Y, Chen Y, *et al*. Eriodictyol inhibits IL-1beta-induced inflammatory response in human osteoarthritis chondrocytes [J]. *Biomed Pharmacother*, 2018, **107**: 1128-1134.
[33] Wei Y, Jia J, Jin X, *et al*. Resveratrol ameliorates inflammatory damage and protects against osteoarthritis in a rat model of osteoarthritis [J]. *Mol Med Rep*, 2018, **17**(1): 1493-1498.
[34] Li B, Jiang T, Liu H, *et al*. Andrographolide protects chondrocytes from oxidative stress injury by activation of the Keap1-Nrf2-Are signaling pathway [J]. *J Cell Physiol*, 2018, **234**(1): 561-571.
[35] Xue EX, Lin JP, Zhang Y, *et al*. Pterostilbene inhibits inflammation and ROS production in chondrocytes by activating Nrf2 pathway [J]. *Oncotarget*, 2017, **8**(26): 41988-42000.

Cite this article as: LIU Mingming, GUO Jiatian, ZHAO Jing, LI Hongye, FENG Xiaoxiao, LIU Haojun, ZHANG Hao, JIA Xuejun, WEI Rushuai, LI Fang, CHEN Chong, HOU Mingzhuang, LV Nanning, XU Haiyan. Activation of NRF2 by celastrol increases antioxidant functions and prevents the progression of osteoarthritis in mice [J]. *Chin J Nat Med*, 2024, **22**(2): 137-145.